Coastal Engineering 176 (2022) 104152

Contents lists available at ScienceDirect

Coastal Engineering

journal homepage: www.elsevier.com/locate/coastaleng

Improved guidance on roughness and crest width in overtopping of rubble mound structures along EurOtop

Mads Røge Eldrup [a,*], Thomas Lykke Andersen [a], Koen Van Doorslaer [b,d], Jentsje van der Meer [c]

[a] Aalborg University, Thomas Manns Vej 23, 9200, Aalborg Øst, Denmark
[b] DEME nv, Scheldedijk 30, 2070, Zwijndrecht, Belgium
[c] Van der Meer Consulting b.v., IHE Delft, PO Box 11, 8491 AA, Akkrum, Netherlands
[d] Ghent University Coastal Engineering Department, Technologiepark 60, 9052, Zwijnaarde, Belgium

ARTICLE INFO

Keywords:
Wave overtopping
Crest width
Wave steepness
Roughness factor

ABSTRACT

In this paper existing guidelines to predict wave overtopping on rubble mound breakwaters and coastal structures are modified and improved with respect to the influence of the roughness and crest width. Data from recently made model tests and existing data are combined to demonstrate the need for modifying these formulations in EurOtop. A new reduction factor γ_{cw} for the crest width is established and is an improvement of the method by Besley. The influence of the roughness of the slope normally include also an influence of the breaker parameter when it is larger than a certain limit (EurOtop suggest $\xi_{m-1,0} > 5$). The present study shows that the breaker parameter is not the ideal dimensionless parameter describing the influence of the wave period for breakwaters with steep slopes, as for such structures the front slope has much less influence on the overtopping than the wave steepness. Thus slope angle and wave steepness have been uncoupled to describe the influence of the armour roughness on wave overtopping. The improvement in the overtopping prediction compared to EurOtop is significant, specifically for the new data sets that have data outside the range of the calibration data used for influence of roughness in EurOtop. The proposed improved methods enlarge the range of applicability with respect to crest width and wave steepness.

1. Introduction

Rubble mound structures are used for protecting ports and coastlines against wave attack. In both cases, a critical design parameter might be the allowable wave overtopping discharge which then dictates the crest level design. There are many structural and sea state parameters that influence the wave overtopping discharge and thus overtopping prediction is complicated. Based on physical model test data, several empirical formulae and neural network prediction methods have been developed and might be used for the crest design of these rubble mound structures. EurOtop (2018) gives the main guidance at present.

Neural networks use many dimensionless input parameters to describe the given structure and the wave climate. A significant advance in overtopping neural networks was provided by the CLASH EU project as a homogenous database with more than ten thousand overtopping model tests was established and used to train neural networks, cf. Van Gent et al. (2007). This database has been further extended in EurOtop (2018) and used to establish improved neural networks on even more data (over 13,000 tests), cf. Formentin et al. (2017). Recently, den Bieman et al. (2021) used the machine learning method XGBoost developed by Chen and Guestrin (2016) to develop a new type of wave overtopping prediction tool. Biemann *et al.* (2021) shows that the XGBoost method reduces the uncertainty on the data used in the paper compared to existing empirical and Neural Network prediction methods. Neural Networks and the XGBoost methods are sometimes referred to as "black boxes" as there is no information on how each parameter influences the predicted wave overtopping discharge. However, the prediction methods are often reliable if trained on a sufficiently large and homogenous database covering all relevant combinations of dimensionless parameters. Using these methods in areas with little or no training data might though provide unreliable results and results that are not physically possible to explain. Such results are often given with a large standard deviation and should then of course be used with caution. But in fact this is not different then applying an empirical formula

* Corresponding author.
E-mail addresses: mrel@build.aau.dk (M.R. Eldrup), tla@build.aau.dk (T. Lykke Andersen), van.doorslaer.koen@deme-group.com (K. Van Doorslaer), jm@vandermeerconsulting.nl (J. van der Meer).

https://doi.org/10.1016/j.coastaleng.2022.104152
Received 17 December 2021; Received in revised form 5 April 2022; Accepted 29 May 2022
Available online 2 June 2022

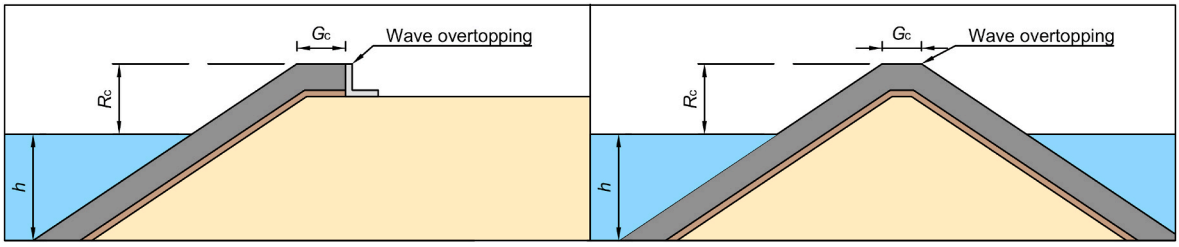

Fig. 1. Definition of crest freeboard, R_c, and crest width, G_c for the present paper. Left shows the definition for a coastal structure with a crown wall. Right shows the definitions for a breakwater without a crown wall.

outside its range of application.

Empirical methods have a narrower validated range of application (smooth slopes, rubble mound or vertical) compared to Neural Network prediction methods, with fewer dimensionless parameters. EurOtop (2018) includes prediction formulae that cover most typical structures and wave climates. EurOtop (2018) includes work from many authors that have improved the predictions step by step by fitting new expressions for different structural layouts and wave conditions through the last decades. Christensen et al. (2014) found that EurOtop (2007) was underpredicting the overtopping for low steepness waves for steep rock armoured structures. They proposed to use a varying roughness factor that is changing with the breaker parameter $\xi_{m-1,0}$, to be used in EurOtop (2007), to improve the predictions. Based on this modification, Eldrup and Lykke Andersen (2018) recalibrated the roughness factors for different armour units. Other test data became available at Ghent university by De Meyere and Vantomme (2017) and De Keyzer and De Kimpe (2018), indicating that the influence of crest width on wave overtopping may differ from the expression by Besley (1999), also given in EurOtop (2018).

The objective of the current paper is to combine new test data from Aalborg University and Ghent University with the existing data in EurOtop (2018) and improve the prediction method for wave overtopping discharge on rubble mound structures, specifically for the influence of roughness and crest width. Section 2 introduces the available data that is used to evaluate the current prediction method in Section 3 and to establish the improved description of the influence of roughness and crest width in Sections 4 and 5. Section 6 evaluates the influence of the armour type on the roughness factor and in Section 7 the final improved equation for the roughness factor is established. Section 8 compares the model test data with the wave overtopping discharges predicted with the present method. Finally, the conclusions on the current work are given in Section 9.

2. Available data

A database from existing model tests with large variation in crest width and freeboard, wave steepness and front slope angle has been established for the present paper. The database includes both structures without a crown wall and with a crown wall. For the case with a crown wall only the case where the top of the wall is at the same level as the armour crest is considered. Fig. 1 shows the coastal structure and breakwater setups used for the present paper and the definitions of crest width and crest freeboard. Note that overtopping at the structure without a crown wall was measured at the rear shoulder. Thus the overtopping trough the permeable crest is not measured and this is also the reason for the used R_c value.

Lowe (1991) investigated the influence of crest width on wave overtopping for rock armour units and this work was continued by Besley (1999). Besley (1999) tested rubble mound structures with rock and accropode armour units. Based on these tests, he established an exponential expression of the crest width to wave height ratio for the influence of the crest width on the overtopping discharge. The coefficients in this exponential expression is dependent on the armour type (rock or accropode). The crest width reduction factor for rock armour is also given as Eq. 6.8 in EurOtop (2018).

Bruce et al. (2009) investigated the influence of the armour unit type (9 different types) on wave overtopping. The work by Bruce et al. (2009) covers a typical range of wave steepness 0.02–0.06 with front slope angles of 1.5 and 2, giving breaker parameters in the range of 2.0–4.6. Bruce et al. (2009) found a small influence from the wave steepness on the roughness factor, but due to the limited tested range in wave steepness, the influence was not found to be significant. The data by Bruce et al. (2009) is now used in the EurOtop (2018) to describe the roughness factor of different armour units.

Geeraerts and Willems (2004) provides data from a gentle rock armoured slope with a fairly large crest width. This data can be used to investigate if the influence of the crest width is different for breaking and non-breaking waves on the structure.

Table 1
Range of parameters for used databases. Wave conditions refer to those at the toe of the structure.

Database	Relative crest width, G_c/H_{m0}	Relative crest height, R_c/H_{m0}	Relative water depth, h/H_{m0}	Front slope angle, cotα	Breaker parameter, $\xi_{m-1,0}$	Wave steepness, $s_{m-1,0}$	Number of tests
Lowe (1991)	0.00–4.98	0.59–1.34	2.62–4.63	2	2.20–3.38	0.022–0.052	70
Besley (1999)	0.00–4.76	0.87–1.88	1.66–1.87	2	2.25–2.42	0.043–0.049	25
Geeraerts and Willems (2004)	1.31–2.41	0.65–2.14	1.68–3.62	4	1.18–2.45	0.010–0.045	142
Bruce et al. (2009)	0.00–2.17	0.62–4.20	5.52–20.96	1.5, 2	2.04–4.59	0.021–0.062	366
Lykke Andersen and Burcharth (2009)	0.93–2.30	0.65–1.76	3.25–9.63	2	2.13–3.51	0.020–0.055	42
De Meyere and Vantomme (2017)	0.45–4.47	0.54–1.61	2.95–9.72	1.5	3.31–8.33	0.006–0.041	65
De Keyzer and De Kimpe (2018)	0.56–5.18	0.53–1.50	3.63–9.38	1.5	3.50–8.33	0.006–0.036	56
Eldrup et al. (2018)	1.18–2.98	1.68–2.09	2.80–3.48	2	2.60–7.08	0.005–0.037	24
Eldrup and Lykke Andersen (2018)	0.66–1.48	1.06–3.74	1.96–4.73	1.5, 2, 3	1.77–9.82	0.005–0.042	98
							888

Lykke Andersen and Burcharth (2009) includes variation in wave steepness, obliquity, directional spreading and a large variation in the dimensionless crest freeboard for rock and cube armour units. This dataset is only used for further verification of the developed methodology for crest and steepness influence, and thus only data for long-crested waves head-on to a rock armoured breakwater is used.

The above described data will be extended in the present section to cover a wider range of the wave steepness and dimensionless crest width and freeboard to tests the applicability of the EurOtop (2018) outside the range it was calibrated to. For this, new data from Ghent University and Aalborg University are used.

The new data from Ghent University (UG) by De Meyere and Vantomme (2017) and De Keyzer and De Kimpe (2018) includes rock and HARO armour units and a large variation in crest width and wave steepness. This data also include lower dimensionless freeboards than those tested by Besley (1999). Thus it may be used to extend the dataset of Besley (1999) for crest width influence and the dataset by Bruce et al. (2009) for influence of large breaker parameters.

New tests performed at Aalborg University (AAU) by Eldrup et al. (2018) and Eldrup and Lykke Andersen (2018) cover rock armoured slopes with a significant variation in front slope angle and wave steepness, and thus the influence of the roughness factor from wave steepness and front slope angle can be investigated separately. The front slope angle and the wave steepness have a much larger variation compared to the work by Bruce et al. (2009). In these data state-of-the-art procedures have been followed to correctly generate and analyse nonlinear waves as needed for the highly nonlinear long waves, cf. Lykke Andersen et al. (2016, 2018) and Eldrup and Lykke Andersen (2019a, 2019b).

The range of tested parameters for all the presented data is shown in Table 1.

3. Evaluation of EurOtop

The overtopping prediction formulae in EurOtop (2018) include various influence factors γ to describe different structural layouts and wave parameters and separated into plunging and surging wave formulae with a transition point between them at $\xi_{m-1,0} = 1.8$ when $\gamma_b = 1$ and $\gamma_v = 1$. EurOtop does not use the term plunging and surging waves, but instead breaking and non-breaking waves on the structure slope itself. The terms spilling, breaking and non-breaking waves are in other publications sometimes describing the type of waves on the foreshore, but in EurOtop they describe the interaction of the waves with the structure. As the present paper is an update of EurOtop their terminology is followed.

For rubble mound structures, the following expression can be given, which provides the EurOtop (2018) procedure for the mean value approach, including the crest width reduction factor C_r and varying roughness factor γ_{fS}. The first part of Eq. (1) is for breaking waves and the second part is for non-breaking waves.

$$\frac{q}{\sqrt{gH_{m0}^3}} = \frac{0.023}{\sqrt{\tan(\alpha)}}\gamma_b\xi_{m-1,0}\exp\left(-\left(2.7\frac{R_c}{\xi_{m-1,0}H_{m0}\gamma_{fS}\gamma_\beta\gamma_b\gamma_v}\right)^{1.3}\right)C_r,$$

With a maximum of: (1)

$$\frac{q}{\sqrt{gH_{m0}^3}} = 0.09\exp\left(-\left(1.5\frac{R_c}{H_{m0}\gamma_{fS}\gamma_\beta}\right)^{1.3}\right)C_r,$$

Here q is the average overtopping discharge per meter width at the crest rear shoulder (see Fig. 1), g is the acceleration of gravity, H_{m0} is the spectral significant wave height. γ_{fS} is the reduction factor for the roughness and permeability of the armour layer including the wave steepness influence (surging waves) from Eq. (4). The effect of wave obliquity is given by γ_β; γ_b includes the effect of a berm; γ_v includes the effect of a vertical wall on the slope; and C_r includes the effect of the crest width, see Eq. (2).

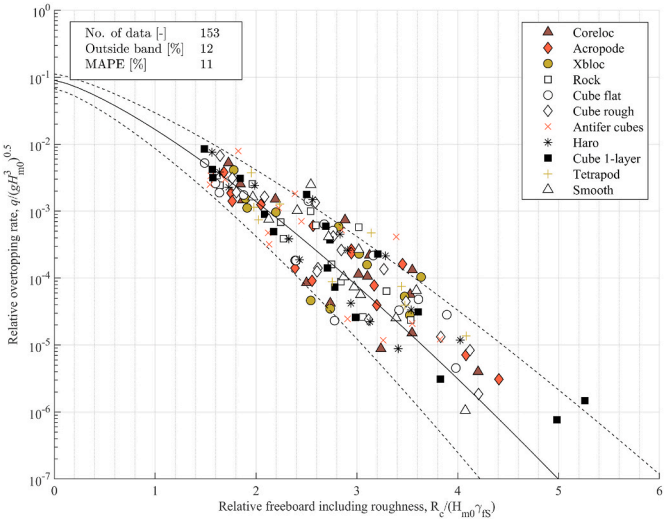

Fig. 2. Modified Fig. 6.7 of EurOtop (2018) for the non-breaking formula in Eq. (1) with 90% confidence band. The horizontal axis includes the roughness factor. Data by Bruce et al. (2009) with cot(α) = 1.5, $\xi_{m-1,0} > 1.8$ and $G_c > 0$ separated into armour unit type.

For all used data in the present paper, either no crown wall is present or it is at the armour crest level and thus R_c is in the present paper taken at the armour crest level A_c. However, the cases with and without the crown wall cannot be compared directly as water passes through the permeable crest when there is no crown wall, which might not be included in the measured overtopping.

The influence of the crest width can presently be calculated with the formula by Besley (1999) with coefficients for rock slopes, also given in EurOtop (2018) as Eq. 6.8.

$$C_r = \min\left(3.06\exp\left(-1.5\frac{G_c}{H_{m0}}\right), 1\right) \quad (2)$$

Here G_c is the width of the crest. The equation shows that if the crest width (G_c) is larger than $0.75H_{m0}$, overtopping will reduce exponentially.

In EurOtop (2007), the influence of low steepness waves (large breaker parameter $\xi_{m-1,0}$) was not included for wave overtopping at rubble mound slopes and thus γ_{fS} equals the roughness factor $\gamma_{fS} = \gamma_f$ (unlike for wave run-up, see Eq. (3)). Christensen et al. (2014) found for rock armoured slopes that the wave overtopping was underpredicted for low steepness waves when using EurOtop (2007). They found a significant improvement in the predictions if the influence of the wave period given for run-up in EurOtop (2007) - (Eq. 6.2) was included also for overtopping. This influence is described by the breaker parameter, $\xi_{m-1,0}$ and given by γ_{fS} in Eq. (3):

for non − breaking waves :

$$\gamma_{fS} = \begin{cases} \gamma_f, & \xi_{m-1,0} < 1.8 \\ \gamma_f + \left(\xi_{m-1,0} - 1.8\right)\left(1 - \gamma_f\right)/8.2, & 1.8 < \xi_{m-1,0} < 10 \\ 1, & \xi_{m-1,0} > 10 \end{cases} \quad (3)$$

for breaking waves :

$$\gamma_{fS} = \gamma_f$$

A slightly different breaker parameter influence was proposed in EurOtop (2018, Eq. 6.7) and given in Eq. (4). The main reason was that influence factors for roughness for all kind of armour units and rock were derived for breaker parameters in the range $\xi_{m-1,0} = 2.0$–4.6, which is a fairly narrow range (Bruce et al., 2009). In this range, the influence factor γ_{fS} showed to be fairly constant, although there was a slight tendency that larger wave periods gave slightly larger overtopping

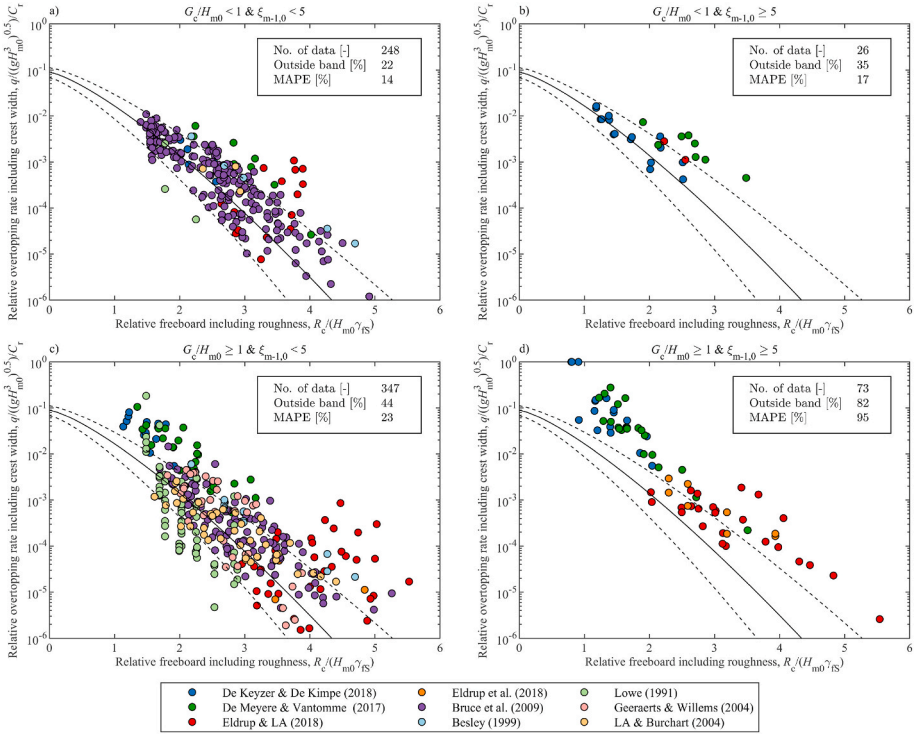

Fig. 3. Comparison of EurOtop (2018) non-breaking formula in Eq. (1) for data with $\xi_{m-1,0} > 1.8$ and separated into short and long waves and narrow and wide crests.

discharges. It was therefore decided by EurOtop (2018) to modify γ_{fS} only if the breaker parameter would exceed a value of 5.

$$\gamma_{fS} = \begin{cases} \gamma_f, \ \xi_{m-1,0} < 5 \\ \gamma_f + (\xi_{m-1,0} - 5)(1 - \gamma_f)/5, \ 5 < \xi_{m-1,0} < 10 \\ 1, \ \xi_{m-1,0} > 10 \end{cases} \quad (4)$$

Fig. 2 shows the original data by Bruce et al. (2009) as in EurOtop (2018) (original Fig. 6.7), but with the roughness factor included in the relative freeboard. The graph shows that nearly all data is within the 90% confidence band. Therefore, it is expected that data with the same tested range as Bruce et al. (2009) will be within the 90% confidence band. This will be examined for the new data defined in Section 2. Furthermore, the Mean Absolute Percentage Error (MAPE) is calculated, where the error of the non-dimensional overtopping has been taken as the error on $\log(q/(gH_{m0}^3)^{0.5})$. The MAPE value together with the percentage of data outside the 90% confidence band are given in Figs. 2 and 3 for comparison.

Fig. 3 compares the prediction by EurOtop (2018) on all the datasets defined in Section 2. The data by Bruce et al. (2009) have narrow crests ($G_c/H_{m0} < 1$) and fairly short waves ($\xi_{m-1,0} < 4.5$ with a wave steepness $s_{m-1,0} > 0.02$) on slopes with front slope cot$\alpha = 1.5$–2, so new data in this range is expected to be within the 90% confidence band. As shown in Fig. 3a most of the data with narrow crests ($G_c/H_{m0} < 1$) and short waves ($\xi_{m-1,0} < 5$) are actually within the 90% confidence band. A few new data points are deviating in that graph from the data by Bruce et al. (2009). The data by Eldrup and Lykke Andersen (2018), that is underestimated in the graph, has breaker parameters in the range $2.7 < \xi_{m-1,0} < 3.5$. The breaker parameter is inside the range of applicability, but the front slope is much more gentle with cot$\alpha = 3$ and smaller wave steepnesses $0.009 < s_{m-1,0} < 0.015$ when compared with the tested range by Bruce et al. (2009).

Fig. 3b presents the data with narrow crests ($G_c/H_{m0} < 1$) and fairly long waves ($\xi_{m-1,0} \geq 5$) and shows that most of the data is within the confidence band, but with a small tendency of underprediction. Fig. 3c presents the data with wide crests ($G_c/H_{m0} \geq 1$) and fairly short waves ($\xi_{m-1,0} < 5$). Part of the new data show a large underprediction by the equation with many of the data outside the confidence band. Some of the datasets have a gentler slope, much larger relative crest widths and a smaller relative freeboard $R_c/(H_{m0}\gamma_{fS})$ compared to what was tested by Bruce et al. (2009). Fig. 3d presents the data with wide crests ($G_c/H_{m0} \geq 1$) and long waves ($\xi_{m-1,0} \geq 5$). The new data show a large underprediction by the equation with most of the data outside the confidence band. Two data points are located at a relative overtopping discharge of 1 on the y-axis which is due to a very low C_r value. It can be concluded that the new data that extends the tested conditions by Lowe (1991), Besley (1999) and Bruce et al. (2009) shows a significant underprediction by EurOtop (2018) for wide crests and low wave steepness.

4. Influence of the crest width

The analysis above shows that the dimensionless wave overtopping discharge for steep slopes depends on the dimensionless crest freeboard, a varying roughness factor (γ_{fS}) that on its turn depends on the armour unit (γ_f), the wave steepness and the front slope angle, and finally depends on the dimensionless crest width if this becomes larger than unity ($G_c/H_{m0} > 1$). Fitting optimized formulae for the influence of the crest width as well as the wave steepness is therefore not straightforward.

The fitting procedure for the two effects adopted here has been separated by first considering data with zero or very small crest widths ($G_c/H_{m0} < 1.1$) where the crest width influence is assumed to be negligible. Based on these data, it is possible to fit γ_{fS} values in narrow intervals of $\xi_{m-1,0}$ for each dataset and front slope. Assuming that γ_{fS} in each $\xi_{m-1,0}$ interval is constant and independent on the crest width, then the same γ_{fS} values for small and large crest widths may be used. Thus it is possible to study the influence of the crest width by using the known γ_{fS} for the data which is obtained from the same dataset, but using only data with narrow crests and identical breaker parameter and front slope. The influence of the crest width is firstly investigated for non-breaking waves which is ensured by only using data with cot$\alpha = 1.5$ and 2.

According to the reduction factor by Besley (Eq. (2)), there is no

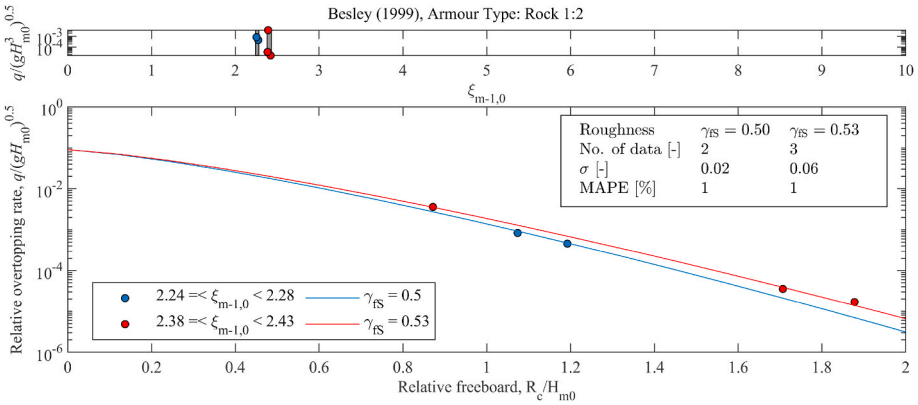

Fig. 4. Example of fitting γ_{fS} for various intervals of $\xi_{m-1,0}$ for narrow crests with $G_c/H_{m0} = 0$. Data of Besley (1999).

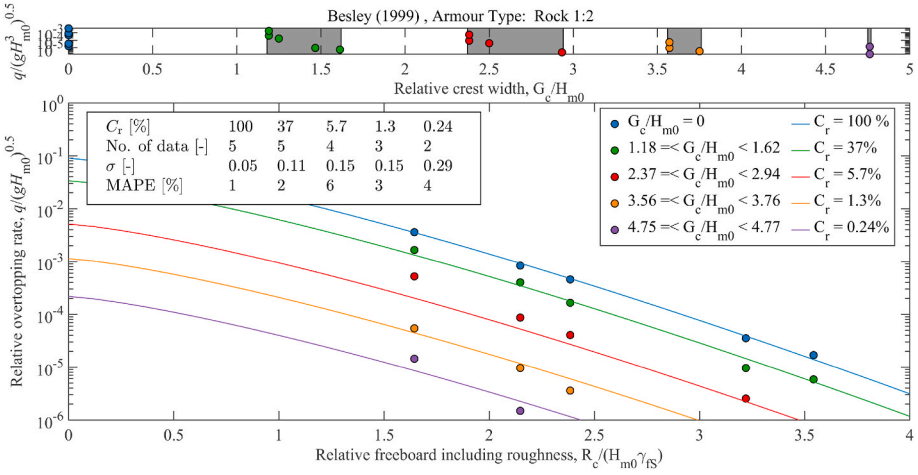

Fig. 5. Influence of crest width and calculated C_r values as given by Besley (1999), Eq. (2), showing a vertical shift of the overtopping curve. Data of Besley (1999).

influence of the crest when $G_c/H_{m0} < 0.75$. Using the strict transition of $G_c/H_{m0} < 0.75$ would limit the available number of data to be used for fitting significantly and thus instead data with $G_c/H_{m0} < 1.1$ is used. This value corresponds to the inclusion of tests which would lead to a reduction in γ_{fS} of 3–8% when using Eq. (1) for $G_c/H_{m0} = 1.1$ and R_c/H_{m0} in the range of 0.9–2.2. This was considered acceptable in order to increase the number of test data. Furthermore, small overtopping discharges are due to a small number of overtopping waves or only spray and thus such data may be less reliable and should be weighted lower in the fitting of γ_{fS}. In the present case it was decided to ignore data with $q/(g\,H_{m0}^3)^{0.5} < 10^{-6}$ in the fitting.

Fig. 4 shows an example of fitting γ_{fS} for the dataset by Besley (1999) with zero crest width ($G_c/H_{m0} = 0$) where a very limited variation in the breaker parameter is found, see the upper graph of Fig. 3. Only two

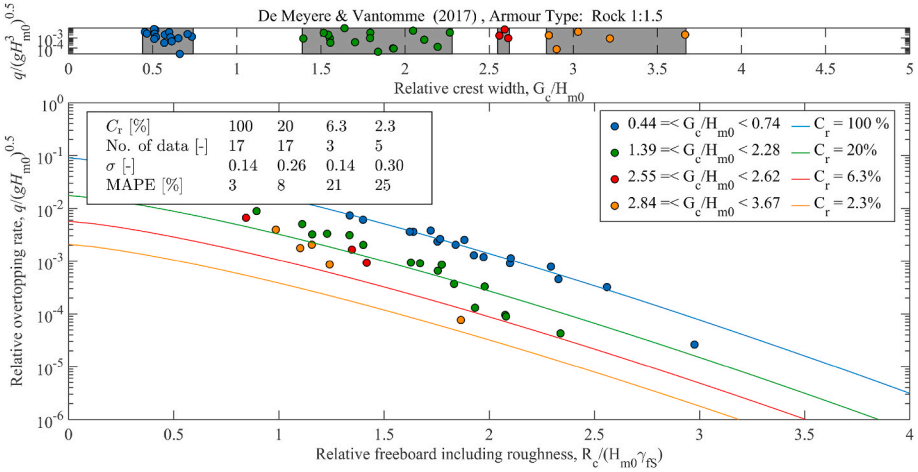

Fig. 6. Influence of crest width and calculated C_r values as given by Besley (1999), Eq. (2), showing increased influence of the crest width with increasing crest freeboard. Data of De Meyere and Vantomme (2017).

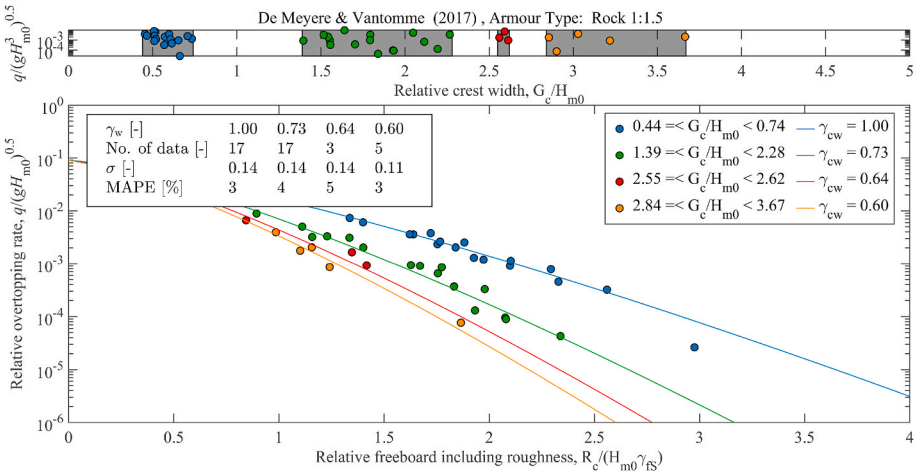

Fig. 7. Fitting a new influence factor γ_{cw} in Eq. (5) for intervals of G_c/H_{m0}. Data of De Meyere and Vantomme (2017).

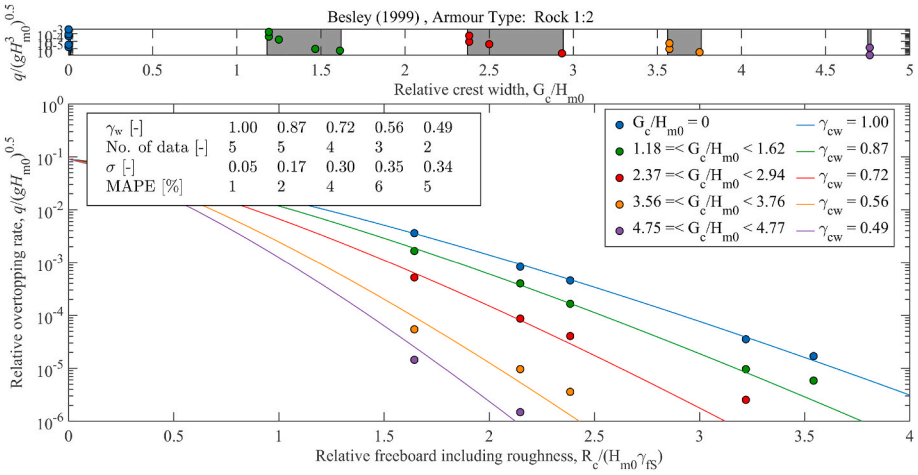

Fig. 8. Fitting a new influence factor γ_{cw} in Eq. (5) for intervals of G_c/H_{m0}. Data of Besley (1999).

classes of breaker parameters are used and they are very close to each other. The lower graph shows the data points in each graph and the fitting. This fitting procedure is generally used for all data sets.

The fitted value of γ_{fS} in these breaker parameter intervals is then assumed to be valid also for wide crests and thus the only unknown is the influence of the crest width itself. Fig. 5 shows all the data by Besley (1999) with $\xi_{m-1,0}$ in the same range of 2.24–2.43 where the fitted γ_{fS} values according to Fig. 4 of 0.50 and 0.53 have been included in the horizontal axis. Note that the two curves in Fig. 4 become one curve with 5 data points in Fig. 5 (upper curve and points). These points belong to a crest width of $G_c/H_{m0} = 0$, see the upper graph of Fig. 5.

Fig. 5 also shows Eq. (1) with calculated values of C_r based on Eq. (2). Note that Eq. (2) is based on the given data set of Besley and described in Besley (1999). Eq. (2) is providing a vertical shift in the predicted overtopping curve. This method fits quite well to the data range of Besley and proves its validity in that range. But for physical reasons it may give a problem for lower freeboards, see the left side of the graph. Fig. 5 and Eq. (2) actually suggest that even if the freeboard is zero (the crest level is equal to the water level), there will be a tremendous effect on overtopping discharge if a wider crest is used. That is not logical as

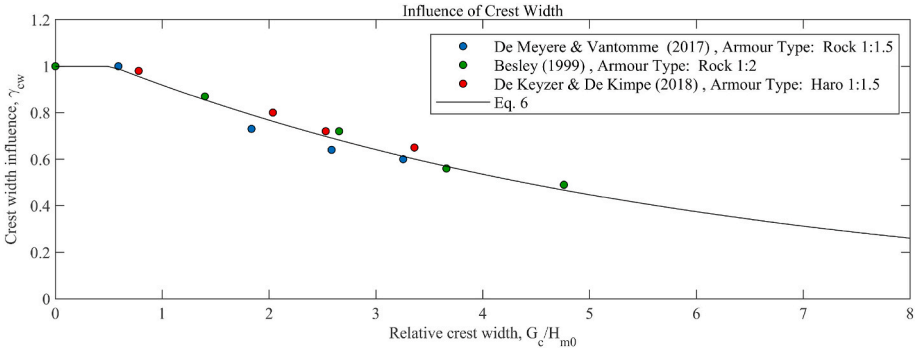

Fig. 9. The new influence factor for the crest width γ_{cw} in Eq. 6, as function of G_c/H_{m0}.

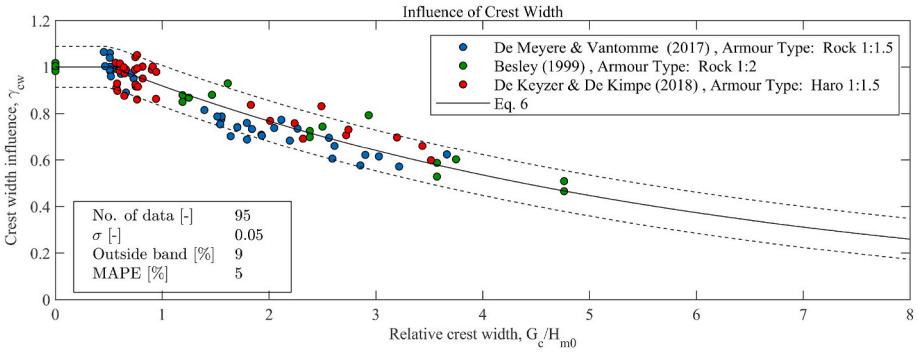

Fig. 10. The influence factor for crest width γ_{cw} as a function of G_c/H_{m0} with all data.

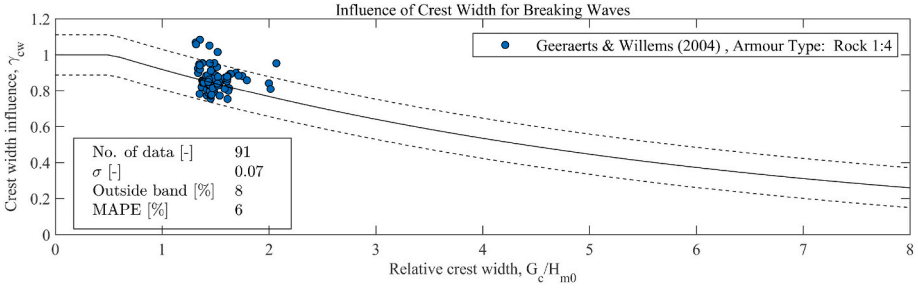

Fig. 11. Influence factors for crest width, γ_{cw} fitted by the breaking waves formula in Eq. (1) on the data by Geeraerts and Willems (2004) with a more gentle slope $\cot\alpha = 4$. The curve shows Eq. 6.

every wave will overtop in such a case, regardless of crest width.

Other datasets, for example the data of De Meyere and Vantomme (2017), do not show a vertical shift, see Fig. 6. There is instead a clear tendency of increasing crest width influence with increasing relative freeboard: the data on the left side in the graph are above the curve and the data on the right side below the curve. Thus the influence of the crest width is not independent on the freeboard as given by the correction factor by Besley. The data in Fig. 6 and also other data sets show that overtopping curves merge for zero freeboard, which is physically sound. Therefore, a new influence factor γ_{cw} is introduced in the EurOtop (2018) formula (Eq. (1)) for non-breaking waves. Instead of C_r as a direct influence on q, γ_{cw} is given in relationship to the relative freeboard R_c/H_{m0}:

$$\text{for non} - \text{breaking waves}:$$

$$\frac{q}{\sqrt{gH_{m0}^3}} = 0.09\exp\left(\left(-1.5\frac{R_c}{H_{m0}\gamma_{fS}\gamma_{cw}\gamma_\beta}\right)^{1.3}\right) \tag{5}$$

The new influence factor γ_{cw} in the modified EurOtop (2018) formula Eq. (5) fits much better with the data by De Meyere and Vantomme (2017), see Fig. 7. The influence factor γ_{cw} is also fitting well to the data by Besley (1999), see Fig. 8 and at least as good as the original fit with Eq. (2): compare Fig. 5 with Fig. 8.

With the fitted values of γ_{cw} it is possible to establish an expression

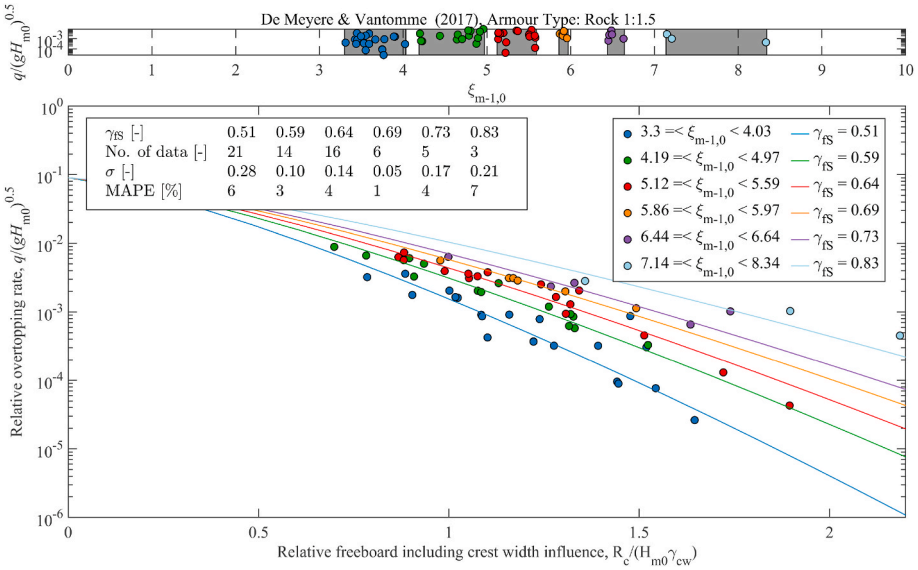

Fig. 12. Example of fitting γ_{fS} for intervals of $\xi_{m-1,0}$ with all G_c/H_{m0} values on the data by De Meyere and Vantomme (2017). Rock slope 1:1.5.

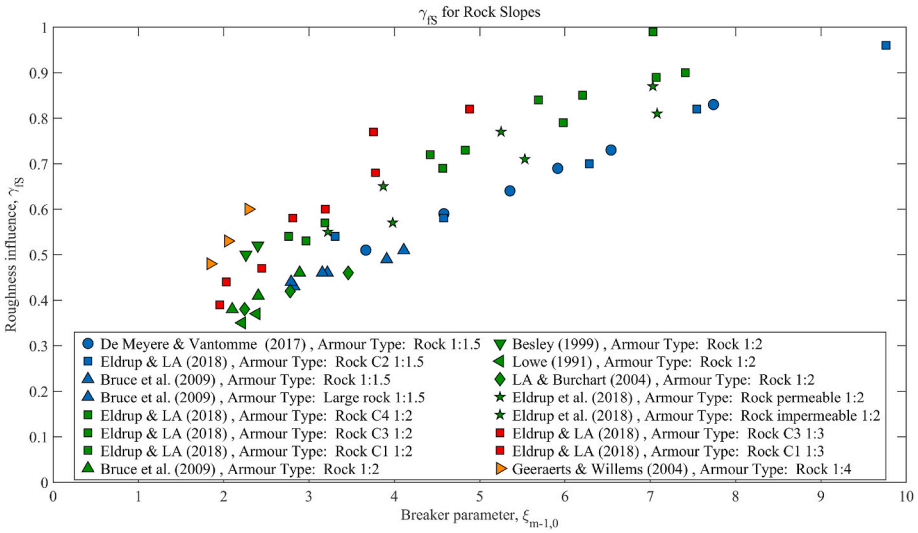

Fig. 13. Influence of breaker parameter $\xi_{m-1,0}$ on γ_{fS} for various slope angles and all data sets.

for the new influence factor for the crest width γ_{cw}, which is dependent on G_c/H_{m0} only. Fig. 9 shows the data points obtained from the trendlines plotted in Figs. 7–8. Furthermore, data by De Keyzer and De Kimpe (2018), which has HARO armour units instead of Rock, has been plotted in Fig. 9 by using the same procedure as in Figs. 7–8. Also the fitted expression for γ_{cw} is shown in the graph and is given in Eq. (6).

$$\gamma_{cw} = \min\left(1.1 \exp\left(-0.18\frac{G_c}{H_{m0}}\right), 1\right) \tag{6}$$

So far, the analysis has been made by trendlines in selected intervals of G_c/H_{m0}. To show the variability in the data, all data points are plotted in Fig. 10, which shows some scatter in each dataset, but Eq. 6 for γ_{cw} is still properly describing the average trend.

The analysis has studied waves with $\xi_{m-1,0} > 1.8$ only, which corresponds to non-breaking waves on the structure when the slopes were steep with $\cot\alpha = 1.5$ and $\cot\alpha = 2$ and that γ_b and $\gamma_v = 1$. A limited part of the collected data is in the breaking waves domain with a slope angle of $\cot\alpha = 4$ and $\xi_{m-1,0} < 1.8$, which can be used to verify if Eq. (6) is also valid for breaking waves on the structure. The formula for breaking waves in Eq. (1) does not include a varying influence factor for roughness, but assumes $\gamma_{fS} = \gamma_f$, see Eq. (3). Note though that the breaking waves formula has an influence of the wave period through the breaker parameter. The data by Geeraerts and Willems (2004) is for rock armour placed with a slope $\cot\alpha = 4$ on top of a core containing fine material and thus it is reasonable to assume that the structure has a γ_f value in between a permeable and impermeable rock structure, according to the values given in EurOtop (2018). An average value between permeable and impermeable rock slopes of $\gamma_f = 0.475$ shows in Fig. 11 an

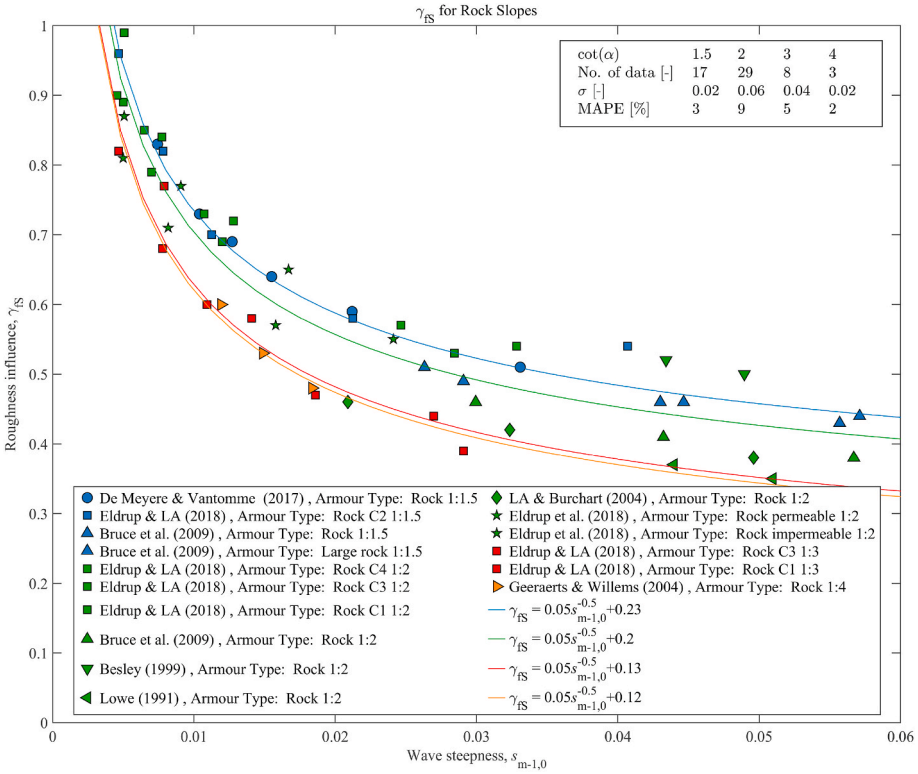

Fig. 14. Influence of wave steepness $s_{m-1,0}$ on γ_{fS} for various slope angles and all data sets for rock armour.

acceptable fit to Eq. (6). Fig. 11 indicates that the crest width influence given by Eq. (6) might also be used for breaking waves in Eq. (1), but the trend is of course not confirmative and should be validated for a wider range of relative crest widths.

5. Wave period and front slope influence

EurOtop (2018) shows that the influence of the wave period is correctly implemented in the breaking waves formula, but for non-breaking waves a varying γ_{fS} is needed and EurOtop (2018) is not describing this correctly, cf. Fig. 3b, d. The separate influence of the wave period (or wave steepness) is investigated here with the objective to improve the formula for γ_{fS}. Earlier studies assumed that the wave period influence on γ_{fS} was governed by $\xi_{m-1,0}$ as used for run-up. Therefore, γ_{fS} is fitted to the different datasets which are separated into front slope and armour type. As in the previous section, γ_{fS} is fitted into intervals of $\xi_{m-1,0}$ and only considering $q/(gH_{m0}^3)^{0.5} > 10^{-6}$, but now with no limitations on crest width (G_c/H_{m0}) as this effect is now known and included in γ_{cw} in Eq. (6). Fig. 12 shows an example of the fitting of γ_{fS} for a 1:1.5 rock structure and with large $\xi_{m-1,0}$. The upper graph shows the intervals of the breaker parameter and the lower graph the overtopping data with the fitted curves. Fitted values of γ_{fS} are given in the legend of the graph. Similar graphs were made for each data set, giving narrow ranges of $\xi_{m-1,0}$ with a fitted γ_{fS} for a specific slope angle and armour unit type.

The relationship between γ_{fS} and $\xi_{m-1,0}$ for all datasets with rock armoured slopes is shown in Fig. 13. EurOtop (2018) uses $\xi_{m-1,0}$ as the governing parameter and reaches a maximum value of $\gamma_{fS} = 1$ for $\xi_{m-1,0} = 10$. Fig. 13 shows a clear separation of the data depending on the breakwater front slope (colour), which means that the breaker parameter alone does not describe the correct effect (if it did, the data for different slope angles would merge). The combined effect of wave steepness and the front slope is not according to the breaker parameter and it is better to analyse them separately.

A similar analysis is performed as for Fig. 13, but instead of using the breaker parameter, the front slope and wave steepness $s_{m-1,0}$ are used, see Fig. 14. The ranges of breaker parameter as in the upper graph of Fig. 12 have been transferred to ranges in wave steepness for a specific front slope. The same fitted γ_{fS} values were used to create Fig. 14.

Fig. 14 clearly shows that for long waves and therefore small wave steepness, say $s_{m-1,0} < 0.02$, the influence of wave steepness is significant. For steeper waves, larger wave steepness, the influence becomes much smaller. The influence factors in EurOtop (2018) for various armour units including rock were based on the work of Bruce et al. (2009), see also Fig. 2. The data points of those tests for a rock structure are also given in Figs. 13 and 14 (with blue Δ for cotα = 1.5) and show an average $\gamma_{fS} = 0.45$ while Bruce et al. (2009) found it to be 0.40. The reason for this difference is that the current analysis has included the influence of the crest width. Those data have an average $G_c/H_{m0} = 1.32$ and using Eq. (6), a $\gamma_{cw} = 0.87$ is obtained, and by multiplying γ_{fS} with γ_{cw}, a total γ value of 0.39 is obtained, which is close to the expected value of 0.40. Thus it seems that the γ_f found in Bruce et al. (2009) are slightly biased due to the influence of the crest width.

EurOtop (2018) mentions that there is a slight tendency of increasing overtopping with increasing wave period, but as the difference was considered small a fixed γ_f was proposed for $\xi_{m-1,0} < 5$. Also Fig. 14 validates that assumption, but it is clear that with all the new data with smaller wave steepness it is better to develop an improved relationship. The data can be described with a power function:

$$\gamma_{fS} = 0.05 s_{m-1,0}^{-0.5} + b \tag{7}$$

where b is a function of the front slope angle. The curves have the same shape but move vertically with different b-value. Scatter for each front slope exists, which might be due to the different permeabilities of the tested breakwaters or other uncertainties that do exist when combining multiple datasets. The scatter for cotα = 1.5 is rather small but, for example, cotα = 2 have data from many sources and it shows a more significant scatter.

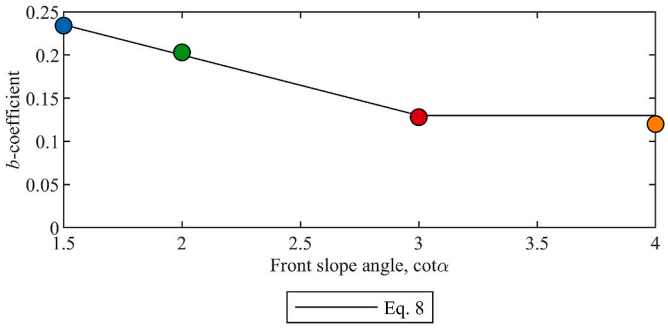

Fig. 15. Influence of the slope angle on the b-coefficient for rock slopes and proposed Eq. (8).

The permeability of the structure (the size of underlayer(s) and core) is expected to influence the b-coefficient, certainly for (very) low wave steepness and a permeable (breakwater), or impermeable core with a thin underlayer (embankment). But the data do not show a consistent trend on this and further studies on the influence of the permeability should be performed to get a better knowledge on this effect. For now, the influence of permeability of the structure has to be ignored.

Based on the above analysis, it is thus assumed that for a rock slope, b mainly depends on the front slope angle, as shown in Fig. 15:

$$b = 0.34 - 0.07 min(\cot(\alpha), 3) \tag{8}$$

This gives for γ_{fS} (for rock structures):

$$\gamma_{fS} = 0.05 s_{m-1,0}^{-0.5} + 0.34 - 0.07 min(\cot(\alpha), 3) \tag{9}$$

The upper value of γ_{fS} is taken as the value for a smooth slope $\gamma_{fS} = 1$.

6. Influence of armour type

So far, the influence of the wave period or wave steepness and slope angle has been analysed for rock slopes only and a further relationship should be established for various concrete armour units. To include the armour type, b-coefficients have been derived using Eq. (7) and fitted for each armour unit as tested by Bruce et al. (2009). Fig. 16, shows the fitting of the b coefficient for concrete armour units tested by Bruce et al. (2009) with cot(α) = 1.5.

The graph shows that the curve is fitting well with the data when using different values of the b-coefficient. The b-coefficient is between 0.18 and 0.30 with the lowest value of 0.18 for tetrapods, while the remaining units are 0.24–0.30. The value for rock is 0.235 using Eq. (8) with cot(α) = 1.5.

In Eqs. (8) and (9) the constant 0.34 is specific for rock slopes and is depending on the b-coefficient. So, the constant 0.34 in Eq. (9) may become a variable c in order to describe the influence of unit type. This gives:

$$\gamma_{fS} = \min\left(0.05 s_{m-1,0}^{-0.5} + c - 0.07 min(\cot(\alpha), 3), 1\right) \tag{10}$$

Here c is depending on the armour type. The influence of the armour unit type (c) should then be a function of γ_f given in EurOtop (2018) Table 6.2. The coefficient c is the only unknown coefficient which can be calculated from Eq. (11) using the fitted b-coefficients shown in Fig. 16.

$$c = b + 0.07 min(\cot(\alpha), 3) \tag{11}$$

Fig. 17 shows the c-coefficients compared to the γ_f values given in EurOtop (2018) and repeated here for the tested unit types by Bruce et al.(2009). The figure shows that the best fit between c and γ_f is described with the linear function $c = \gamma_f$ - 0.09. The reason for the offset value of 0.09 will be explained in the next section.

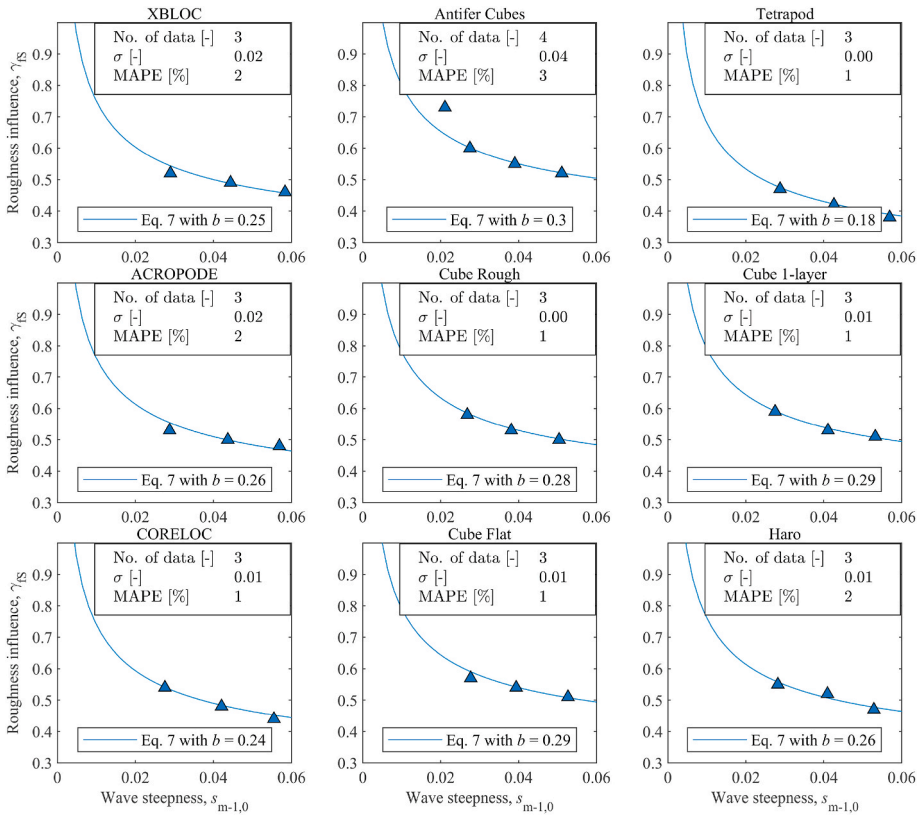

Fig. 16. Influence of $s_{m\text{-}1,0}$ on γ_{fS} for concrete armour units with a front slope of 1:1.5 tested by Bruce et al. (2009).

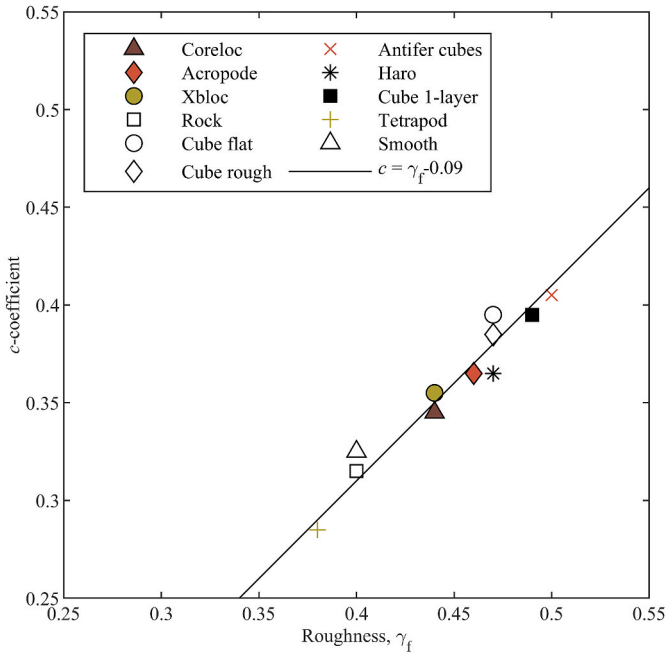

Fig. 17. The coefficient c for Bruce et al. (2009) data compared to γ_f from EurOtop (2018).

7. Final influence factor for roughness

Combining Eq. (10) with Eq. (11) gives the final expression for γ_{fS}. The present study includes wave steepness down to $s_{m\text{-}1,0} = 0.005$, but in very shallow water it can be even smaller. For lower wave steepness the upper limit of $\gamma_{fS} = 1$ in Eq. (12) would typically be reached. Therefore, the validity of Eqs. (5) and (12) has not been verified for very shallow water conditions. For rock armour the formula has been validated on $1.5 \leq \cot\alpha \leq 4$, but for concrete armour units the procedure has only been validated for $\cot\alpha = 1.5$. For concrete armour units the slope is very often 1:1.5, but for for single layer interlocking units it may be even

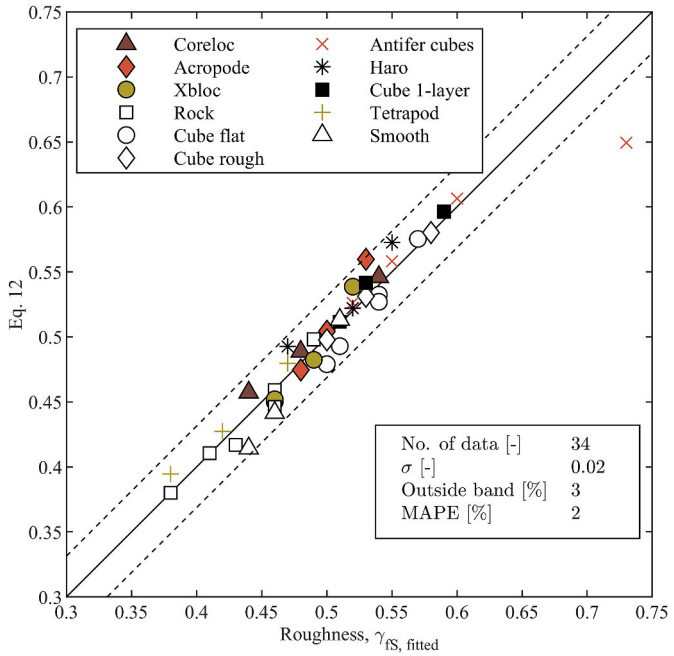

Fig. 18. Calculated and fitted values of γ_{fS} using for Bruce et al. (2009) data.

Table 2
Roughness factors γ_f for permeable rubble mound structures from EurOtop (2018), Table 6.2.

	EurOtop
Armour	γ_f
Rocks (2 layers)	0.40
Rocks (2 layers large)	0.40
Rocks (2 layers with impermeable core)	0.55
Cubes (1 - layer)	0.49
Cubes (2 – layer flat)	0.47
Cubes (2 – layer rough)	0.47
Antifers	0.50
HARO's	0.47
Tetrapods	0.38
Accropode™ I	0.46
Xbloc®	0.44
CORE-LOC®	0.44

steeper and for massive units like cubes it may be flatter and for such units 1:2 is quite typical. The expression becomes:

$$\gamma_{fS} = \min\left(\gamma_f + 0.05 s_{m-1,0}^{-0.5} - 0.07 min(\cot(\alpha), 3) - 0.09, 1\right) \quad (12)$$

Eq. (12) is valid for all types of armour units and slope angles. For a slope angle of 1:1.5, Eq. (12) reduces to:

$$\gamma_{fS} = \min\left(\gamma_f + 0.05\, s_{m-1,0}^{-0.5} - 0.195,\ 1\right) \quad (13)$$

The investigation by Bruce et al. (2009) had an average wave steepness of $s_{m\text{-}1,0} = 0.042$ and they tested structures with an average value of $\gamma_f = 0.45$. By applying Eq. (13) with these values, a $\gamma_{fS} = 0.50$ is found. This increase in the reduction factor is explained by the new crest width factor γ_{cw} that was introduced in this study. Bruce et al. (2009) did not include the influence of the crest width in their analysis, but their tests have an average value over all the tests with all kind of armour units of $G_c/H_{m0} = 1.27$. By using Eq. (6) is obtained $\gamma_{cw} = 0.88$, which is close to the observed ratio for $\gamma_f/\gamma_{fS} = 0.9$. Thus it can be concluded that the γ_f values reported by Bruce et al. (2009) is influenced by the crest width, using the new proposed equation for crest width. Theoretically, this crest width influence may be removed and new roughness factors could be established. This would then lead to a different offset value in Eq. 9. Such approach is not really improving the application of roughness factors and therefore the original γ_f values from EurOtop (2018) will be used with the offset value of 0.09 in Eq. (12).

Fig. 18 shows a comparison between the fitted γ_{fS} on the data by Bruce et al. (2009) and the calculated value using Eq. (12) with the γ_f value from Table 2 (a part of the original Table 6.2 in EurOtop (2018)).

8. Evaluation of modified formula against all data

The predictions with the new influence factors for crest width and roughness are obtained using Eqs. (6) and (12) respectively in the modified overtopping Eq. (5). The roughness factors (γ_f) given by EurOtop (2018), which have also been given in Table 2, are used for the calculations. Using the new influence factors also means that the transition point between the breaking and non-breaking waves formulae changes as γ_{fS} is no longer equal to γ_f for $\xi_{m\text{-}1,0} < 5$ and that γ_{cw} so far is only included in the non-breaking waves formula. Further data is needed to validate γ_{cw} for the breaking waves formula. The number of data points in Fig. 19 might deviate from the number of data points found in Fig. 3 due to the different transition point between the formulae.

The use of the newly established reduction factors is shown for all the used data for non-breaking waves in Fig. 19. Comparing Fig. 19 with the predictions by EurOtop (2018) in Fig. 3, it is clear that the predictions in Fig. 19 have improved significantly. Data with wide crests ($G_c/H_{m0} > 1$) and long waves ($\xi_{m\text{-}1,0} > 5$) are no longer underpredicted, but are mainly within the 90% confidence band. Furthermore, the scatter is reduced in every of the data groups.

9. Conclusions

This paper gives an improved method to incorporate the influence of crest width and wave period (wave steepness) on wave overtopping over rubble mound structures with a steep slope, resulting in non-breaking

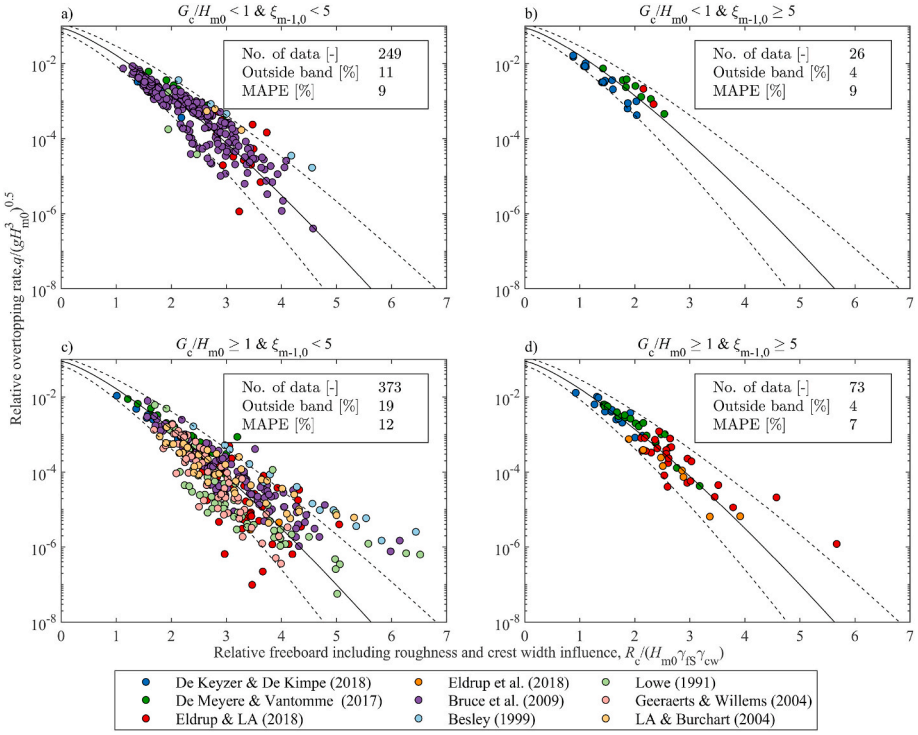

Fig. 19. Evaluation of Eqs. (5), (6) and (12) and separated into short and long waves and narrow and wide crests.

waves on the structure. The original data of Bruce et al. (2009) were used as they describe many different types of armour units. Moreover, new data sets were added with wide crests and also with low wave steepness, both inside and outside the range of the data by Bruce et al. (2009) and the resulting equations in EurOtop (2018).

The method by Besley (1999) to describe the influence of crest width has been improved, using his own data as well as new data. The main change was to connect the influence factor directly to the relative crest height and not as a reduction factor on the overtopping discharge. In this way, a zero crest height becomes independent of the crest width, which is physically more sound. Eq. (2) has been replaced with Eq. (6) which gives the modified influence factor for crest width Eq. (6) has been validated on data with a relative crest widths in the interval $0 \leq G_c/H_{m0} \leq 5.18$.

The analysis on wave steepness and slope angle for non-breaking waves showed that the breaker parameter is not the best parameter to describe their influence on wave overtopping. The influence of wave period or wave steepness is much larger than the influence of the slope angle, and the definition of the fixed relationship in the breaker parameter shows not to be adequate enough. Therefore, the wave steepness and front slope have been treated separately. The trend of the influence of wave steepness on wave overtopping for steep slopes with non-breaking waves can be described by a power function, regardless of armour unit type. Low wave steepness (long wave period) has a much more significant effect on overtopping than higher steepness. The final influence depends on the armour type, by means of a relationship with the fixed influence factors for various units as in EurOtop (2018). Eq. (4) has been replaced with Eq. (12), which gives the expression for the wave steepness and front slope angle influence factor. Eq. (12) has been validated for front slope angles $1.5 \leq \cot(\alpha) \leq 4$ and wave steepness $0.005 \leq s_{m-1,0} \leq 0.062$.

The equation for wave overtopping for rubble mound slopes and non-breaking waves as in EurOtop (2018) was modified slightly to include the new/modified influence factors γ_{cw} for crest width and γ_{fS} for roughness, wave steepness and front slope angle. The formula for non-breaking waves in Eq. (1) has been replaced with Eq. (5). Due to the fitting on new data inside and outside the existing ranges of applicability, the proposed method improves the description of influence of crest width and wave steepness on wave overtopping significantly.

CRediT authorship contribution statement

Mads Røge Eldrup: Conceptualization, Methodology, Model testing, Formal analysis, Visualization, Writing – original draft. **Thomas Lykke Andersen:** Conceptualization, Methodology, Formal analysis, Writing – review & editing. **Koen Van Doorslaer:** Conceptualization, Methodology, Model testing, Formal analysis, Writing – review & editing. **Jentsje van der Meer:** Conceptualization, Methodology, Formal analysis, Writing – review & editing.

Declaration of competing interest

The authors declare that they have no known competing financial interests or personal relationships that could have appeared to influence the work reported in this paper.

References

Besley, P., 1999. Wave Overtopping of Seawalls, Design and Assessment Manual. R&D Technical Report W178. https://repository.tudelft.nl/islandora/object/uuid:0cd1c50d-0957-4599-aa37-e6328da73988?collection=research.

Bruce, T., van der Meer, J.W., Franco, L., Pearson, J.M., 2009. Overtopping performance of different armour units for rubble mound breakwaters. Coast Eng. 56 (2), 166–179. https://doi.org/10.1016/j.coastaleng.2008.03.015.

Chen, T., Guestrin, C., 2016. XGBoost: a scalable tree boosting system. In: Proceedings of the ACM SIGKDD International Conference on Knowledge Discovery and Data Mining, 13-17-August-2016. https://doi.org/10.1145/2939672.2939785.

Christensen, N.F., Røge, M.S., Thomsen, J.B., Andersen, T.L., Burcharth, H.F., Nørgaard, J.Q.H., 2014. Overtopping on rubble mound breakwaters for low steepness waves in deep and depth limited conditions. Proc. Coast. Eng. Conf.

De Keyzer, A., De Kimpe, T., 2018. The Influence of Crown Walls on Wave Overtopping for Concrete Armour Unit Breakwaters. Experimental Modelling. Ghent University.

De Meyere, G., Vantomme, L., 2017. The Influence of Crown Walls on Wave Overtopping over Rubble Mound Structures. Experimental Modelling. Ghent University.

den Bieman, J.P., van Gent, M.R.A., van den Boogaard, H.F.P., 2021. Wave overtopping predictions using an advanced machine learning technique. Coast Eng. 166 https://doi.org/10.1016/j.coastaleng.2020.103830.

Eldrup, M.R., Andersen, T.L., 2019a. Applicability of nonlinear wavemaker theory. J. Mar. Sci. Eng. 7 (1) https://doi.org/10.3390/jmse7010014.

Eldrup, M.R., Andersen, T.L., 2019b. Estimation of incident and reflected wave trains in highly nonlinear two-dimensional irregular waves. J. Waterw. Port, Coast. Ocean Eng. 145 (1) https://doi.org/10.1061/(ASCE)WW.1943-5460.0000497.

Eldrup, M.R., Lykke Andersen, T., 2018. Recalibration of overtopping roughness factors of different armour types. In Coasts, Mar. Struct. Breakwaters 1011–1020. https://doi.org/10.1680/cmsb.63174.1011, 2017.

Eldrup, M.R., Andersen, T.L., Thomsen, J.B., Burcharth, H.F., 2018. Overtopping on breakwaters with a permeable crest. Coast. Eng. Proceed. 1 (36) https://doi.org/10.9753/icce.v36.papers.17.

EurOtop, Pullen, T., Allsop, N.W.H., Bruce, T., Kortenhaus, A., Schüttrumpf, H., Van der Meer, J.W., 2007. Wave Overtopping of Sea Defences and Related Structures: Assessment Manual. www.overtopping-manual.com.

EurOtop, Van der Meer, J.W., Allsop, N.W.H., Bruce, T., De Rouck, J., Kortenhaus, A., Pullen, T., Schüttrumpf, H., Troch, P., Zanuttigh, B., 2018. Manual on Wave Overtopping of Sea Defences and Related Structures an Overtopping Manual Largely Based on European Research, but for Worldwide Application. www.overtopping-manual.com.

Formentin, S.M., Zanuttigh, B., Van der Meer, J.W., 2017. A neural network tool for predicting wave reflection, overtopping and transmission. Coast Eng. J. 59 (1) https://doi.org/10.1142/S0578563417500061, 1750006-1-1750006–1750031.

Geeraerts, J., Willems, M., 2004. Final Report on Laboratory Measurements on the Ostia Case.

Lowe, J.P., 1991. Report EX 2310.

Lykke Andersen, T., Burcharth, H.F., 2009. Three-dimensional investigations of wave overtopping on rubble mound structures. Coast Eng. 56 (2), 180–189. https://doi.org/10.1016/j.coastaleng.2008.03.007.

Lykke Andersen, T., Clavero, M., Frigaard, P., Losada, M., Puyol, J.I., 2016. A new active absorption system and its performance to linear and non-linear waves. Coast Eng. 114, 47–60. https://doi.org/10.1016/j.coastaleng.2016.04.010.

Lykke Andersen, T., Clavero, M., Eldrup, M.R., Frigaard, P., Losada, M., 2018. Active absorption of nonlinear irregular waves. In: Proceedings of the Coastal Engineering Conference.

Van Gent, M.R.A., Van den Boogaard, H.F.P., Pozueta, B., Medina, J.R., 2007. Neural network modelling of wave overtopping at coastal structures. Coast Eng. 54 (8), 586–593. https://doi.org/10.1016/j.coastaleng.2006.12.001.